Original Article

The Influence of Signal to Noise Ratio on the Pharmacokinetic Analysis in DCE-MRI Studies

Azimeh NV Dehkordi *, Saeideh Koohestani

Department of Physics, Najafabad Branch, Islamic Azad University, Najafabad, Iran

Received: 26 October 2019
Accepted: 15 December 2019
DOI: 10.1039/x0xx00000x
http://FBT.tums.ac.ir

Keywords:
Dynamic Contrast Enhanced-MRI;
Signal to Noise Ratio;
Pharmacokinetic Parameters Accuracy;
Contrast Concentration Uncertainty.

Abstract

Purpose: Recruiting the Pharmacokinetic (PK) parameters estimated from non-invasive methods such as Dynamic Contrast Enhanced MRI (DCE-MRI) to evaluate or plan treatment procedure is widely investigated in clinical practices. Interpretation of the DCE-MRI data is highly dependent to precision and accuracy of the estimated parameters. One of the most effective factors on the DCE-MR images and on the contrast concentration profile is the Signal to Noise Ratio (SNR). This work focuses on the analytical evaluation of the noise effect on accuracy of the estimated PK parameters in DCE-MRI studies.

Materials and Methods: Tofts model as a popular pharmacokinetic model and model selection technique was used to simulate 3470 time curves of contrast concentration. Maximum likelihood estimator as a minimum variance unbiased estimator was recruited to estimate the PK parameters. Eleven levels of signal to noise ratios (SNR= 5, 8, 10, 13, 15, 20, 25, 30, 35, 50, Noiseless) were added to the simulated CA concentration profiles. The PK parameters were estimated for 11 series data and then Mean Percentage Error (MPE) was calculated for estimated parameters.

Results: The results indicate that the most sensitive parameter to the SNR of the DCE-MR images is inverse transfer constant. A SNR greater than 25 was found to ensure a reasonable error (MPE <5%) in all models parameters.

Conclusion: Clinical decision based on the DCE-MRI data analysis and estimated PK parameters needs a good image quality (SNR>25), an accurate and robust estimator and correct pharmacokinetic model selection.

1. Introduction

Pharmacokinetic analysis of Dynamic Contrast Enhanced MRI (DCE-MRI) has a wide application in clinical practices [1-5]. Good accuracy and reproducibility of these parameters is essential when they are used as a marker for treatment evaluation or treatment planning. Accuracy and precision of the Pharmacokinetic (PK) parameters in DCE-MRI studies is challenged by different sources of error such as error in quantification of Arterial Input Function (AIF) [6-10], low signal to noise ratio of images [9, 11], mis-specification in pulse sequence parameters [11, 12], tissue intrinsic properties [5, 13], pharmacokinetic model selection [14], scan time duration [6], temporal resolution [9, 12] and contrast agent rate [6, 7]. Since the PK parameters estimation in DCE-MRI is totally signal-starved, thus noise can change the value of the estimated PK parameters by influencing on the DCE-MRI signals. Signal to Noise Ratio (SNR) that measured as averaged signal intensity to standard deviation [15] by affecting on the time Contrast Agent (CA) concentration profile can be one important factor in bias of estimated PK parameters [13, 16, 17]. Noise can affect time-CA concentration profiles and consequently affect the pharmacokinetic model fitting and thereby causes error in PK parameters. Thus, effects of SNR on

Corresponding Author:
Azimeh NV Dehkordi, PhD
Department of Physics, Najafabad Branch, Islamic Azad University, Najafabad, Iran
Tel: (+98)913 3847617
Email: noorizadeh.az@gmail.com

the accuracy and precision of the PK parameters is an important issue that a few recent literature investigated it [9, 11, 13, 16]. The magnetic field strength, slice thickness, filed of view and pulse sequence parameters can affect the signal to noise ratio. In the literature, optimizing the scan parameters and scan time has been considered to improve the signal to noise ratio and reduce the kinetic parameters error [9]. A few researchers also studied the optimum SNR to have the best accuracy for the estimated PK parameters [9, 11, 16, 18]. For example, Kershaw *et al.* [9] studied the optimum SNR and time resolution to have the bias less than 5% in parameters of the AAHT Model. Naeyer *et al.* [11] investigated the propagation of the noise from time-MR signal onto processing steps via extended Tofts model and consequently to PK parameters uncertainty. Schabel and Parker *et al.* [13] formulated the effect of the noise on the measured concentration values. As far as we know, there is no research that has analytically investigated the trend of the noise effect on the estimated PK parameters and has quantified the influence of the different SNRs on the error value and error rate of the estimated PK parameters in DCE-MRI studies. In this work, using the extended Toft's model as one of the common and popular pharmacokinetic model and recruiting a recently developed MLE algorithm [1, 4, 19, 20], the error of the estimated PK parameters affected by different SNRs in DCE-MR images was analytically evaluated and quantified

2. Materials and Methods

2.1. The Noise Effect on the Contrast Concentration Measurement

In DCE-MRI technique, the time changes of the CA concentration are measured and tissue physiological properties such as blood plasma volume (vp), transfer rate between vasculature and interstitial space (K^{trans} and kep) and extravascular extracellular space (ve) are estimated according to the measured time varying signal. These pharmacokinetic parameters can be useful in diagnostic and evaluating tumors situations, stroke tissue etc. [2-4]. In DCE-MRI and Spoiled Gradient Echo pulse (SPGRE) sequence, the MR signal intensity according to the scan parameters can be formulated as following [13]:

$$S(T_1.T_2^*) = M_0 \frac{\sin\alpha(1-e^{-T_R/T_1})e^{-T_E/T_2^*}}{1-e^{-T_R/T_1}\cos(\alpha)} \quad (1)$$

In this Equation, α is flip angle, TR is repetition time, TE is echo time and M_0 is equilibrium magnetism, T1 is longitudinal relaxation time and T_2^* is transverse relaxation time. Injection of the contrast agent enhances the MR signal intensity. Subtraction of the signal intensity after contrast injection ($S=S(T_1 \llbracket .T \rrbracket_{2}^{*})$) from signal intensity before injection of the CA (base signal) ($S(T_{1.0} \llbracket .T \rrbracket_{2.0}^{*})$) relate to the base signal results the relative enhancement of the MR signals [11, 13]:

$$\mu = \frac{S(T_1.T_2^*) - S(T_{1.0}.T_{2.0}^*)}{S(T_{1.0}.T_{2.0}^*)} \quad (2)$$

$T_{1.0}$ and $T_{2.0}^*$ are native longitudinal and transverse relaxation times (before injection), respectively. Schabel and Parker [13] showed that the variance of μ can be calculated according to the variance of S and S_0:

$$var(\mu) = var(S)\left(\frac{\partial\mu}{\partial S}\right)^2 + var(S_0)\left(\frac{\partial\mu}{\partial S_0}\right)^2 = \frac{{S_0}^2 var(S) + S^2 var(S_0)}{{S_0}^2} \quad (3)$$

Since var(S) is variance of the signal S, which defines as $(S_0/SNR)^2$ and var(S_0) is variance of the base signal, which defines as S_0/N_B, thus above equation can be rewritten as following form [13]:

$$var(\mu) = var(S)\frac{(S^2 + N_B {S_0}^2)}{N_B {S_0}^4} \quad (4)$$

NB is imaging repetition number before contrast agent injection. By fusion of the above Equations a complete formula can be achieved for variance of measured contrast concentration based on the variance of the signal enhancement [13]:

$$var(C.\mu) = \frac{1}{SNR^2}\left(\frac{1}{\beta}\right)^2 (E_1 cos\alpha - 1)^4 \left(\frac{1}{N_B}\left(\frac{E_1 - 1}{E_1 cos\alpha - 1}\right)^2 + \left(\frac{E_{1.0} - 1}{E_{1.0} cos\alpha - 1}\cdot\frac{E_{2.0}}{E_2}\right)^2\right) \quad (5)$$

In Equation 5, β, E_1 and E_2 describes as following:

$$\beta = r_1 T_R E_1 (cos\alpha - 1) + r_2 T_E (E_1 - 1)(E_1 cos\alpha - 1) \quad (6)$$

$$E_{1.0} = \exp\left(-\frac{T_R}{T_{1.0}}\right). \qquad E_1 = \exp(-T_R R_1) \quad (7)$$

$$R_1 = R_{1.0} + r_1 C. \qquad R_{1.0} = \frac{1}{T_{1.0}}$$

$$E_{2.0} = \exp\left(-\frac{T_R}{T_{2.0}}\right). \qquad E_2 = \exp(-T_R R_2) \quad (8)$$

$$R_2 = R_{2.0} + r_2 C\,. \qquad R_{2.0} = \frac{1}{T_{2.0}^{*}}$$

In Equations 7 and 8, $R_1=1/T_1$ and $R_2=1/T_2$ are longitudinal and transverse relaxation rate and r_1 and r_2 are longitudinal and transverse contrast relaxivities. As shown in the above Equations, the variance of the measured CA concentration in SPGRE imaging protocol is inversely related to squared SNR. Since, the standard deviation can be calculated from square root of the variance, then increment of the SNR decreases contrast concentration uncertainty. Therefore, for decreasing the uncertainty of the concentration measurement, the SNR should be improved with optimizing the imaging parameters.

In order to investigate the dependency of the measured concentration uncertainty to noise of the DCE-MR images, a wide range of signal to noise ratio was selected (SNRs: 5, 8, 10, 13, 15, 20, 25, 30, 35, 50). The SNR in various imaging centers is different, so the studied SNR range was chosen to cover almost all the common SNRs in clinical brain DCE-MR imaging centers. Several imaging parameters such as field strength, TE and TR values are also needed and assumed as following: field strength=3 T and TE/TR = 0.84/5.8 ms. The intrinsic tissue properties (such as T_1, T_2, $T_{1.0}$, $T_{2.0}$, r_1 and r_2) were considered for three different brain tissues (Blood, Water and Plasma) (Table.1).

Then, using the explained above Equations (Equation 1-8), variance and uncertainty of CA concentration signals was calculated for each signal to noise ratio and three different tissues.

2.1.1. Contrast Concentration Simulation

Assessment of the noise effect on the accuracy of the pharmacokinetic parameters was performed using signal simulation in MATLAB software (MATLAB 2016a, The MathWorks Inc., Natick, MA, 2000). To this order, using the extended Toft's model as a PK model to describe the CA distribution between blood plasma and extravascular extracellular space, 3470 time-concentration signals were simulated with a wide range of pharmacokinetic parameters .The range of the PK parameters was chosen comply to the physical meaningful and prevalent values of these parameters in clinical and literature. Variation of parameters to produce these 3470 signals was summarized in Table 2. Since, the distribution of the contrast agent may confront different conditions in different tissues, thus according to the model selection concept [21], three physiologically nested models were considered and 10 time-concentration profiles for Model 1 (Equation 9), 310 time-concentration profiles for Model 2 (Equation 10) and 3150 time concentration profiles were simulated for Model 3 (Equation 11) [19, 21].

Model 1: $C(t)=v_p C_p(t)$, (9)

Model 2: $C(t)=K^{trans}\int_0^t C_p(\tau).d\tau + v_p C_p(t)$ (10)

Model 3: $C(t)=K^{trans}\int_0^t C_p(\tau).e^{-(k_{ep}(t-\tau)}d\tau + v_p C_p(t)$ (11)

In the above equations, C(t) is time signal of contrast agent in the tissue, $C_p(t)$ is time signal of contrast concentration in blood plasma, v_p is blood plasma volume, K^{trans} and kep are forward and inverse transfer constant between blood plasma and extravascular extracellular space.

Table 1. The tissue intrinsic properties for water, plasma and blood part of the brain in 3T

Tissue	r_1 (mmol^{-1} s^{-1})	r_2 (mmol^{-1} s^{-1})	$T_{1.0}$ (ms)	$T_{2.0}^{*}$ (ms)
Water	3.1	3.7	5000	3125
Plasma	3.7	5.2	2272	344
Blood	3.9	6.9	1900	320

Table 2. Variation of PK parameters for simulating Model 1, 2 and 3 profiles [19]

	v_p	K^{trans}	k_{ep}
Model 1	0.5% to 9.5%	-	-
Model 2	0.5% to 9.5%	0.01 to 0.76 min^{-1}	-
Model 3	0.5% to 9.5%	0.01 to 0.51 min^{-1}	0.035 to 0.735 min^{-1}

Noise of the concentration signal at each voxel has a normal distribution, thus a Gaussian distribution can be assigned to the noise of DCE-MR images. Distribution of the MR signals (S) around its mean value (S_{mean}) can be describe as [11]:

$$f_s = \frac{1}{\sqrt{2\pi\sigma_s}} e^{-\frac{(S-S_{mean})^2}{2\sigma_s{}^2}} \qquad (12)$$

S is MR signal in each repetition; S_{mean} is the mean of the registered MR signals and σ_s is standard deviation.

White Gaussian noise was added to all 3470 simulated time contrast concentration signals (10 signals for Model 1, 310 signals for Model 2 and 3150 signals for Model 3) to prepare 10 signal to noise ratios (mentioned in section 2.1), so 11 data series of each generated signal (1 pure signal and 10 different noisy signals) were produced.

2.1.3. Quantification of the PK parameters Using Maximum Likelihood Estimation

After adding 10 levels of noise, 11 data series were produced (1 pure data series which were simulated at the first step and 10 noisy data series which were generated by adding the different levels of noise to the pure data).

In the next step, pharmacokinetic parameters were estimated for all 11 × 3470 signals. In this study, Maximum Likelihood Estimator (MLE) as an accurate, robust and low bias estimator [11, 19] according to a previously designed algorithm [19, 20] was recruited to estimate the PK parameters.

The main idea of the MLE is finding the parameters value (θ^{ML}) to maximize the observations. In our study, parameters of 3 Equations (9-11) were found by MLE. Subsequently, one parameter for Model 1 (Equation 9), θ^{ML}=[vp], two parameters for Model 2 (Equation10), θ^{ML} =[vp, K^{trans}] and three parameters for Model 3 (Equation11), θ^{ML}=[vp, K^{trans}, kep] were estimated.

In Equations 9-11, C is time-signal of each voxel, thus Ci is concentration value in each voxel at ith time point. Comply with simulated data, a Normal distribution was used as distribution of data probability:

$$C_i \sim f_N(M,\sigma^2) \qquad (13)$$

$$M= E[C], \quad \sigma^2= var(C)$$

$$L_i=\frac{1}{\sqrt{2\pi\sigma^2}} e^{\frac{(Ci-M_i)^2}{2\sigma^2}} \qquad (14)$$

In Equations 13 and 14, σ is standard deviation, M is exception and C is contrast concentration for different Models.

Li is likelihood function constructed for ith time point. Ci is assumed to be an independent variable for different time points during DCE-MR experiment. Thus, for the full DCE-MRI observation, the likelihood function is a product of the individual likelihoods (Equation 15):

$$L=L_i\times L_2\times\cdots\times L_N=\prod_{i=1}^{N} L_i \qquad (15)$$

According to Equation 14 and 15, L can be re-written as bellow (Equation16):

$$L=\left(\frac{1}{\sqrt{2\pi\sigma^2}}\right)^N . e^{\sum_{i=1}^{N}\frac{(y_i-M_i)^2}{2\sigma^2}} \qquad (16)$$

Using the constructed likelihood function in Equation 15 (or log-likelihood form stated in Equation 17), the θ^{ML} can be estimated by taking the derivative from the likelihood function and setting the obtained equations to zero.

$$\ln L=-\frac{N}{2}\ln(2\pi)-\frac{N}{2}\ln(\sigma^2)+\sum_{i=1}^{N}\frac{(y_i-M_i)^2}{2\sigma^2} \qquad (17)$$

2.1.4. Calculation of Mean Percentage Error (MPE) for the Estimated PK Parameters

To evaluate the propagated error in PK parameters affected by change in SNR, the Mean Percentage Error (MPE) of each parameter for each data series was calculated relate to parameters value estimated for noiseless data (Equation 18):

$$MPE_{SNR}=\frac{1}{N}\sum_{k=1}^{N}\left(1-\frac{Est_{SNR}^{k}}{truth_{SNR}^{k}}\right)\times 100 \qquad (18)$$

N refers to the number of profiles in each set. The Est_{SNR}^{k} and $truth_{SNR}^{k}$ are the estimated and the source of truth for each PK parameter, respectively.

3. Results

Figure 1 demonstrates the effect of the noise in DCE-MRI data on the contrast concentration variance and uncertainty at each voxel. Variance and relative uncertainty of contrast concentration versus contrast concentration values in different SNRs and for three tissues (blood, water and plasma) are shown in Figure 1-A to 1-F. It can be seen in Figure 1-A to 1-C that by increasing the concentration value, variance of measured concentration increases; As shown in this figure the variance is almost the same in different SNRs up to 6 mM contrast concentration, but the difference of the calculated variance is observable at higher values of the contrast concentration values; especially at concentration higher than 10 mM.

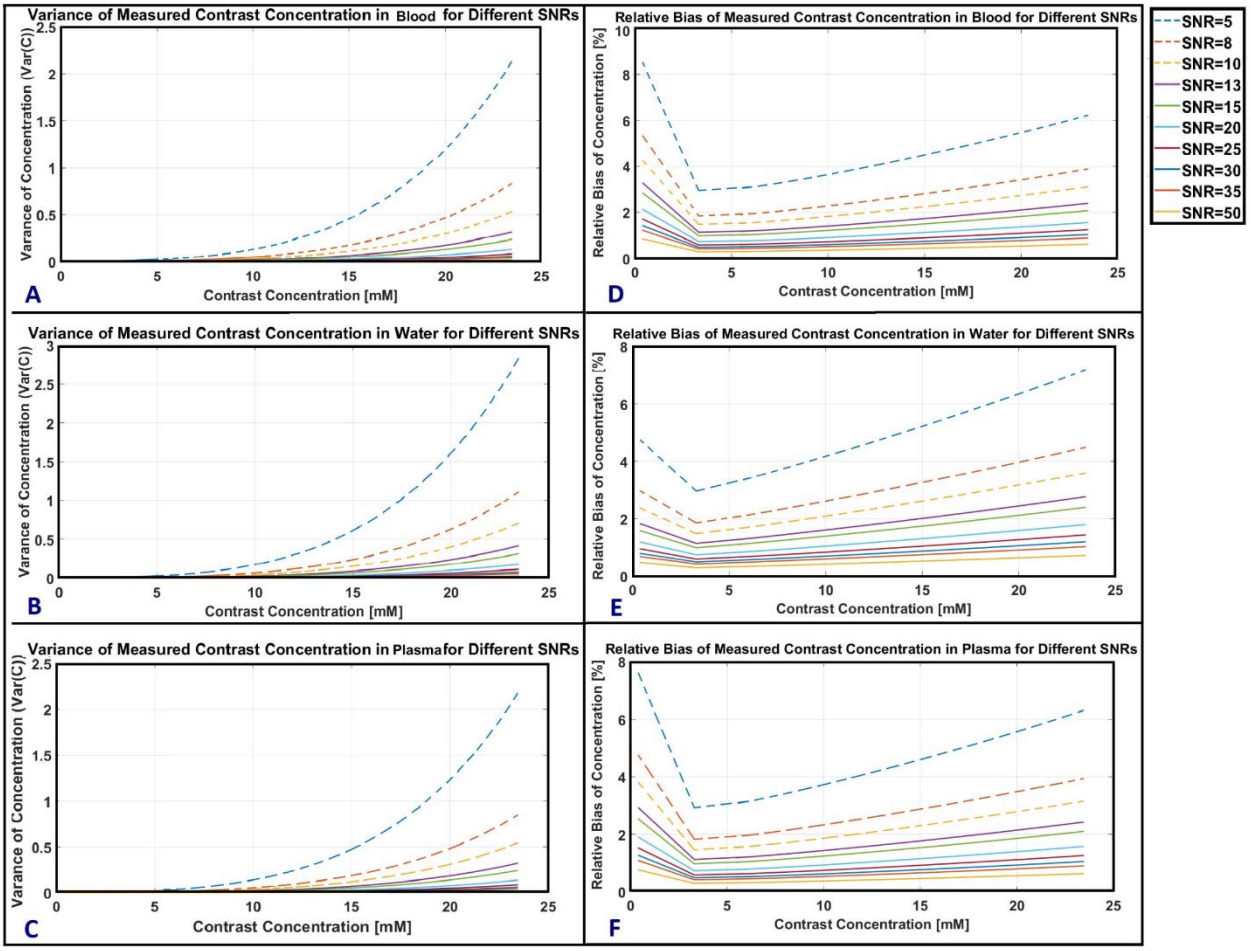

Figure 1. This figure demonstrates the effect of the noise in DCE-MRI data on the contrast concentration variance for A) blood, B) water, and C) plasma tissue. Relative uncertainty of contrast concentration for D) blood, E) water and F) plasma at each voxel

Figure 2 demonstrates the Mean Percentage Error (MPE) for parameter of Model 1(blood plasma volume, vp). This figure shows that MPE of vp is under 1% for all studied SNRs; even it can be under 0.5% for SNRs greater than 20.

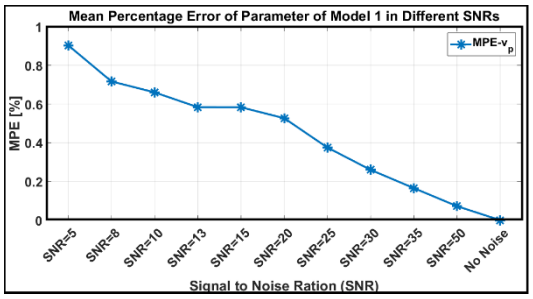

Figure 2. This figure displays the calculated Mean Percentage Error (MPE) of the Blood Plasma Volume estimated for Model 1 of Tofts equation

MPE of the estimated parameters for Model 2 (vp and K^{trans}) is shown in Figure-3. In Figure 3-a it can be observed that MPE is decreasing by increasing the SNR, such that for SNR=5, MPE of vp is significant (~33.5%) while for SNRs more than 20, MPE would be less than 8%. In this figure, it is also shown that the lowest MPE for K^{trans} is occurred at SNR=15, which is around 0.12%, and in worse situation (SNR=5) reach to 5.5%.

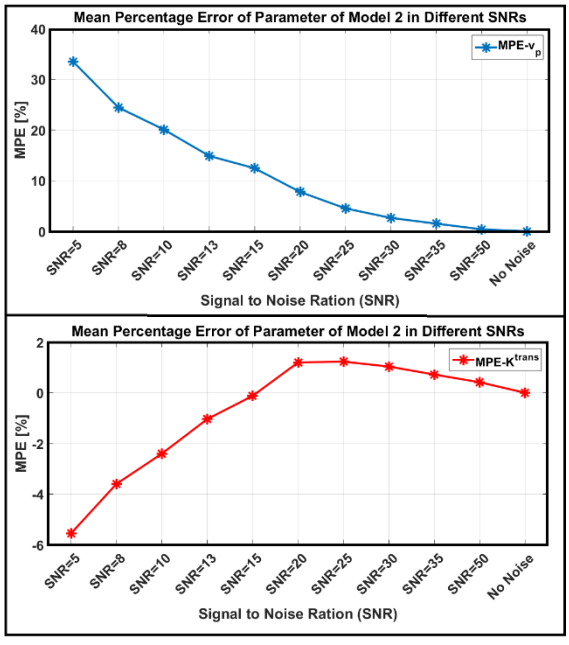

Figure 3. This figure displays the calculated Mean Percentage Error (MPE) of A) the Blood Plasma Volume and B) Forward Transfer Constant estimated for Model 2 of Tofts equation

The results of the calculated MPE for Model 3 parameters for different SNRs are depicted in Figure 4. Among three parameters of Model 3, inverse transfer constant (kep) shows most noise sensitivity and blood plasma volume (vp) shows lowest noise sensitivity; for example, MPE of kep reaches to 52% at SNR=5, while MPE of vp is 4.5% at this SNR. The SNR should be at least equal to 20 to have a MPE under 5% for all three parameters of Model 3.

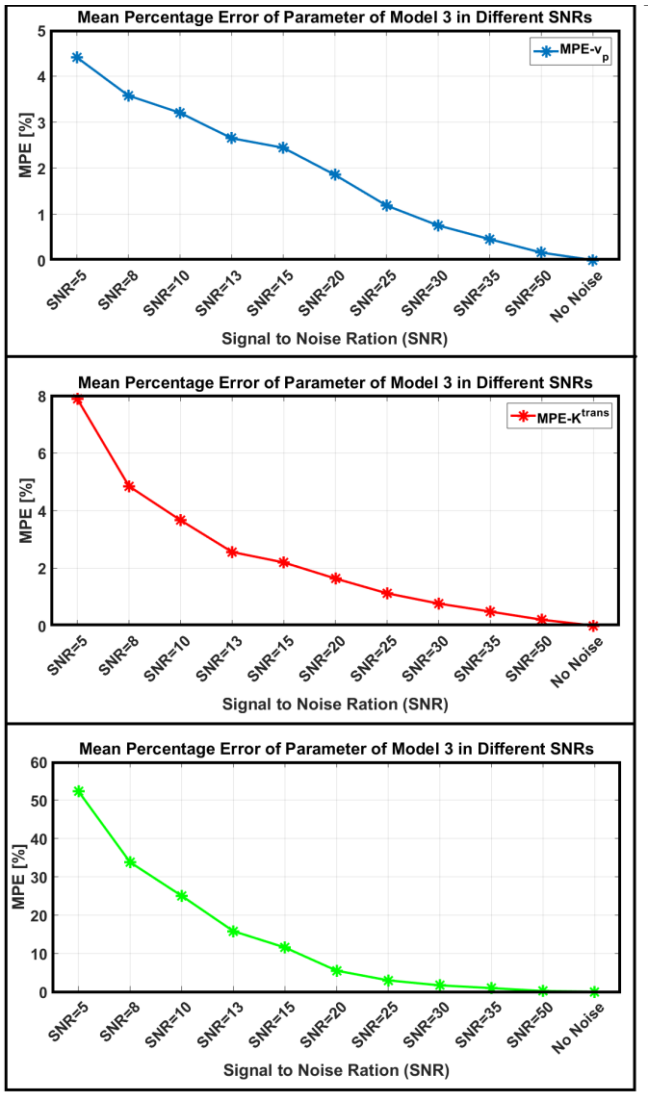

Figure 4. This figure displays the calculated Mean Percentage Error (MPE) of A) the Blood Plasma Volume and B) Forward Transfer Constant C) Inverse Transfer Constant estimated for Model 3 of Tofts equation

Figure 5 exhibits a comparison between the percentage of error increment for plasma volume parameter in three models versus percentage increment of noise. To this order, the MPE in SNR=50 was picked up as base of

comparison and noise increment in other SNRs was computed relate to SNR=50, because MPE of all parameters are almost negligible at SNR=50. As shown in Figure 5, relative MPE (respect to the MPE at SNR=50) for all three models grow with increasing noise. Among three models, vp1 shows low sensitivity to noise enhancement, even if the noise level grows up 900% respect to the SNR=50, the relative MPE of vp1 does not reach to 1%. vp3 is more susceptible than vp1 and vp2, insofar as noise level becomes 2 times (SNR=25) or 10 times (SNR=5) higher, MPE of this parameter will increase up to 10% or 33%, respectively.

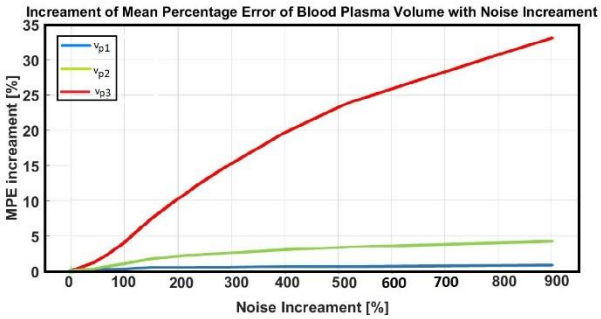

Figure 5. This figure illustrates the changes of the MPE when noise increases relate to noise in SNR=50 for Blood Plasma Volume of 3 Tofts extracted Models

The results of this comparison for forward transfer constants in Model 2 and Model 3 are shown in Figure 6. The significant observation in this figure is that absolute MPE changes of K^{trans} for all noise increments are under 8%. It can be also seen that the noise sensitivity of these two parameters are approximately the same, however the MPE changes are positive for K^{trans3} but it is negative for K^{trans2}.

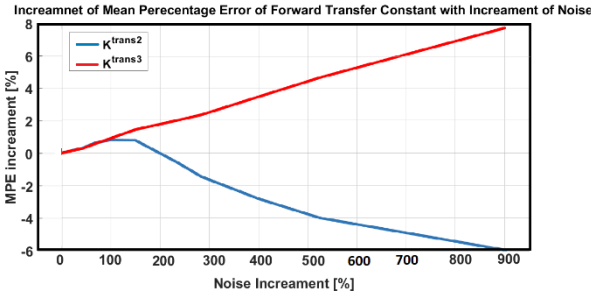

Figure 6. This figure illustrates the changes of the MPE when noise increases relate to noise in SNR=50 for Forward Transfer Constants of Model 2 and 3 extracted from Tofts equation

The MPE changes of the inverse transfer constant (kep) in Model 3 affected by the noise increment are plotted in Figure 7. This figure shows that the most sensitive PK parameter to the noise increment is kep of Model 3. For example, as noise level increases up to 2 or 10 times higher than SNR50, MPE of kep increases 9% or 52%, respectively.

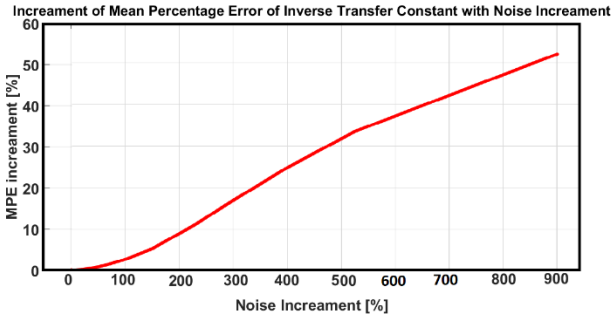

Figure 7. This figure illustrates the changes of the MPE when noise increases relate to noise in SNR=50 for Inverse Transfer Constant of Model 3 extracted from Tofts equation

In addition to MPE that indicates the accuracy of the estimated parameters, Pearson Correlation Coefficient (CC) was also calculated between the true values and estimated values of the PK parameters for all 10 data series. Table-3 lists the calculated CC for all PK parameters in 10 SNRs. As it can be realized from this table, there is a positive relationship between true and estimated values of these parameters in all SNRs; in low SNRs, CC is weak for blood plasma volume of Model 2 and 3 and inverse transfer constant. Whereas, the CC would be higher than 0.87 for all PK parameters in SNRs greater than 30, which confirms the resulted assured SNR (SNR>25) from computed MPE and Figure 2 to 7.

4. Discussion

This study and a few recent investigations [9, 11, 13, 16] show that the noise can significantly affect the precision and accuracy of the pharmacokinetic analysis of the DCE-MRI studies. As Crone *et al.* [22] showed poor quality images (images with low SNR) may cause physiologically meaningless parameters appear. Thus, recruiting the pharmacokinetic DCE-MRI data analysis in clinical decisions should be conditioned to acquire DCE-MR images with high quality (high SNR). Kale *et al.* [23] reported that the most important factor of the image quality is SNR and needed SNR to have the best

Table 2. Correlation Coefficient between Estimated and True value of Pharmacokinetic Parameters in different SNRs

PK parameters	Model 1	Model 2		Model 3		
	vp	vp	K^{trans}	vp	K^{trans}	kep
SNR=5	r=1 p=0	r=-0.10 p=0.07	r=1 p=0	r=0.78 p=0	r=0.99 p=0	r=0.67 p=0
SNR=8	r=1 p=0	r=-0.05 p=0.41	r=1 p=0	r=0.85 p=0	r=0.992 p=0	r=0.73 p=0
SNR=10	r=1 p=0	r=0.001 p=0.98	r=1 p=0	r=0.88 p=0	r=0.995 p=0	r=0.78 p=0
SNR=13	r=1 p=0	r=0.09 p=0.09	r=1 p=0	r=0.93 p=0	r=0.997 p=0	r=0.87 p=0
SNR=15	r=1 p=0	r=0.17 p=0.003	r=1 p=0	r=0.95 p=0	r=0.998 p=0	r=0.94 p=0
SNR=20	r=1 p=0	r=0.41 p=0	r=1 p=0	r=0.98 p=0	r=0.999 p=0	r=0.99 p=0
SNR=25	r=1 p=0	r=0.68 p=0	r=1 p=0	r=0.996 p=0	r=1 p=0	r=0.998 p=0
SNR=30	r=1 p=0	r=0.87 p=0	r=1 p=0	r=0.997 p=0	r=1 p=0	r=0.998 p=0
SNR=35	r=1 p=0	r=0.95 p=0	r=1 p=0	r=0.998 p=0	r=1 p=0	r=0.999 p=0
SNR=50	r=1 p=0	r=0.99 p=0	r=1 p=0	r=0.999 p=0	r=1 p=0	r=0.999 p=0

image quality around 30 to 35 [23]. The results of this study indicate that for having a reasonable accuracy to estimate the PK parameters (MPE <5%), at least a SNR greater than 25 is needed. In a fixed imaging protocol, the MR signal is constant and the noise is not related to the signal [17]. Therefore, the most significant effective factors on the SNR of the DCE-MRI data is electron thermal fluctuations in receiver coils [23]. An important step in improving the images quality and SNR is using developed technology in receiver coil geometry, improved pulse design, high-conductivity materials for receiver coils and advanced image processing methods. Although improving the SNR with optimizing the pulse sequence parameter may sacrifice the spatial resolution of MR images [17, 23], a compromise should be made between the SNR (quality image) and spatial resolution.

The precision of the estimated parameters is highly dependent to the estimation technique. The recruited estimator should not add extra bias or variance to the estimated parameters. According to the literature [24], if there is an unbiased estimator, it should be the maximum likelihood estimator. The results of these studies and previously published researches [11, 24] indicated that the MLE technique as a Minimum Variance Unbiased Estimator (MVUE) is more appropriate and faster technique than other common techniques such as Least Square Error (LSE) to use in DCE-MRI data analysis [11, 19, 20]. The previously published research [11] showed that ML estimator can reduce the uncertainty up to 30% for K^{trans} and up to 20% for ve compared with LSE. Therefore, it also can be said that using the MLE technique, the parameters are estimated without adding extra biases during the estimation process. However, the results of this study depict that MLE is somehow sensitive to noise. If all processing and estimation techniques are the same between various imaging centers, the SNR is usually different among them. Thus recruiting an estimation technique that would be less sensitive to noise than the MLE is more interesting in pharmacokinetic analysis of DCE-MRI data. A previously published paper [19] showed that the adaptive estimation technique can be a good, fast and less noise sensitive substitute for MLE technique.

5. Conclusion

In this study, by recruiting MLE technique, the propagated error in Toft's PK parameters from the noise increment in DCE-MRI signals is analytically investigated. The results of this study denote that most sensitive PK parameters to noise changes is Model 3 parameters, especially inverse transfer constant. Employing the pharmacokinetic analysis for making clinical decision-making criteria needs images with a reasonable quality and also an accurate and robust estimator. The SNR equal or greater than 25 along with maximum likelihood estimation technique were proposed in this study to have mean percentage error less than 5% for all PK parameters.

References

1- A. N. V. Dehkordi *et al.*, "A Fuzzy-Based Model to Predict the Survival Rate of Patients with Glioblastoma Multiforme Tumor," *Neuro-Oncology*, vol. 17, no. 5, p. 166, November 1, 2015 2015.

2- M. P. Aryal *et al.*, "Dynamic Contrast Enhanced MRI Parameters and Tumor Cellularity in a Rat Model of Cerebral Glioma at 7T," *Magn Reson in Med*, vol. 71, no. 6, pp. 2206-2214, 2014.

3- X. Li *et al.*, "Glioma grading by microvascular permeability parameters derived from dynamic contrast-enhanced MRI and intratumoral susceptibility signal on susceptibility weighted imaging," *Cancer Imaging*, vol. 15, no. 1, p. 4, 03/21, 2015.

4- A. N. V. Dehkordi, A. Kamali-Asl, N. Wen, T. Mikkelsen, I. J. Chetty, and H. Bagher-Ebadian, "DCE-MRI prediction of survival time for patients with glioblastoma multiforme: using an adaptive neuro-fuzzy-based model and nested model selection technique," (in eng), *NMR Biomed*, vol. 30, no. 9, Sep 2017.

5- R. B. Ger *et al.*, "A Multi-Institutional Comparison of Dynamic Contrast-Enhanced Magnetic Resonance Imaging Parameter Calculations," *Scientific Reports*, vol. 7, no. 1, p. 11185, 2017/09/11 2017.

6- R. G. Lopata, W. H. Backes, P. P. van den Bosch, and N. A. van Riel, "On the identifiability of pharmacokinetic parameters in dynamic contrast-enhanced imaging," (in eng), *Magn Reson Med*, vol. 58, no. 2, pp. 425-9, Aug 2007.

7- H. J. Aerts, N. A. van Riel, and W. H. Backes, "System identification theory in pharmacokinetic modeling of dynamic contrast-enhanced MRI: influence of contrast injection," (in eng), *Magn Reson Med*, vol. 59, no. 5, pp. 1111-9, May 2008.

8- C. Yang, G. S. Karczmar, M. Medved, A. Oto, M. Zamora, and W. M. Stadler, "Reproducibility assessment of a multiple reference tissue method for quantitative dynamic contrast enhanced–MRI analysis," *Magnetic Resonance in Medicine*, vol. 61, no. 4, pp. 851-859, 2009.

9- L. E. Kershaw and H. L. Cheng, "Temporal resolution and SNR requirements for accurate DCE-MRI data analysis using the AATH model," (in eng), *Magn Reson Med*, vol. 64, no. 6, pp. 1772-80, Dec 2010.

10- Noorizadeh Azimeh, Bagher-Ebadian Hassan, Faghihi Reza, Narang J, Jain rajan, and Ewing James R., "Input Function Detection in MR Brain Perfusion Using a Blood Circulatory Model Based Algorithm," in *International Society of Magnetic Resonance in Medicine*, Stockholm, Sweden, 2010.

11- D. De Naeyer, Y. De Deene, W. P. Ceelen, P. Segers, and P. Verdonck, "Precision analysis of kinetic modelling estimates in dynamic contrast enhanced MRI," (in eng), *Magma*, vol. 24, no. 2, pp. 51-66, Apr 2011.

12- M. Heisen, X. Fan, J. Buurman, N. A. W. van Riel, G. S. Karczmar, and B. M. ter Haar Romeny, "The influence of temporal resolution in determining pharmacokinetic parameters from DCE-MRI data," *Magnetic Resonance in Medicine*, vol. 63, no. 3, pp. 811-816, 2010.

13- M. C. Schabel and D. L. Parker, "Uncertainty and bias in contrast concentration measurements using spoiled gradient echo pulse sequences," (in eng), *Phys Med Biol*, vol. 53, no. 9, pp. 2345-73, May 7 2008.

14- D. L. Buckley, "Uncertainty in the analysis of tracer kinetics using dynamic contrast-enhanced T1-weighted MRI," (in eng), *Magn Reson Med*, vol. 47, no. 3, pp. 601-6, Mar 2002.

15- T. B. Parrish, D. R. Gitelman, K. S. LaBar, and M. M. Mesulam, "Impact of signal-to-noise on functional MRI," (in eng), *Magn Reson Med*, vol. 44, no. 6, pp. 925-32, Dec 2000.

16- X. Li, W. Huang, and W. D. Rooney, "Signal-to-noise ratio, contrast-to-noise ratio and pharmacokinetic modeling considerations in dynamic contrast-enhanced magnetic resonance imaging," (in eng), *Magnetic resonance imaging*, vol. 30, no. 9, pp. 1313-1322, 2012.

17- S. Portnoy, S. C. Kale, A. Feintuch, C. Tardif, G. B. Pike, and R. M. Henkelman, "Information content of SNR/resolution trade-offs in three-dimensional magnetic resonance imaging," *Medical Physics*, vol. 36, no. 4, pp. 1442-1451, 2009.

18- S. R. Barnes, T. S. C. Ng, A. Montagne, M. Law, B. V. Zlokovic, and R. E. Jacobs, "Optimal acquisition and modeling parameters for accurate assessment of low K^{trans} blood–brain barrier permeability using dynamic contrast-enhanced MRI," *Magnetic Resonance in Medicine*, vol. 75, no. 5, pp. 1967-1977, 2016.

19- D. A. N.V., K. A. Alireza, E. J. R., W. Ning, C. I. J., and B. E. Hassan, "An adaptive model for rapid and direct estimation of extravascular extracellular space in dynamic contrast enhanced MRI studies," *NMR in Biomedicine*, vol. 30, no. 5, p. e3682, 2017.

20- H. Bagher-Ebadian, A. Dehkordi, and J. Ewing, "SU-F-I-26: Maximum Likelihood and Nested Model Selection Techniques for Pharmacokinetic Analysis of Dynamic Contrast Enhanced MRI in Patients with Glioblastoma Tumors," *Medical Physics*, vol. 43, no. 6, pp. 3392-3392, 2016.

21- H. Bagher-Ebadian *et al.*, "Model Selection for DCE-T1 Studies in Glioblastoma," *Magnetic Resonance in Medicine*, vol. 68, no. 1, pp. 241-251, 2012.

22- G. O. Cron, Sourbron, S., Barboriak, D., Abdeen, R., Hogan, M.,Nguyen, T.B., and "Bias and precision of three different DCE-MRI analysis software packages: a comparison using simulated data," in *International Society for Magnetic Resonance in Medicine*, 2014, p. 4592.

23- S. C. Kale, X. J. Chen, and R. M. Henkelman, "Trading off SNR and resolution in MR images," *NMR in Biomedicine*, vol. 22, no. 5, pp. 488-494, 2009.

24- Voinov V. G. and N. M.S., "Unbiased estimators and their applications, Vol.1: Univariate case.," vol. 1: *Kluwer Academic Publishers*, 1993, p. 521.

